

Determining Critical Micelle Concentration of Organic Corrosion Inhibitors and its Effectiveness in Corrosion Mitigation

Negar Moradighadi,^{‡,*} Starr Lewis,^{*} Juan Dominguez Olivo,^{*} David Young,^{*} Bruce Brown,^{*} and Srdjan Nešić^{*}

Critical micelle concentration (CMC) of a surfactant corrosion inhibitor is considered to be an important property which may indicate its corrosion mitigation efficiency. One of the common methods to determine a CMC is via surface tension measurements of inhibitor solutions. In this work, the validity of surface tension measurement as an indirect technique for the detection of micelle formation is discussed and tested in conjunction with an alternative method—fluorescence spectroscopy, which was used as a technique that more directly detects micelles in a solution. Results show that surface tension measurements of a quaternary ammonium bromide inhibitor solution, that can determine the concentration at which the water/air interface becomes saturated by the inhibitor molecules, does not always correlate with the formation of micelles. In some cases, the formation of micelles occurred in the same concentration range while in others it happened at much higher concentrations, as determined by fluorescence spectroscopy. Moreover, there was no clear correlation between CMC and maximum inhibition of the corrosion rate.

KEY WORDS: adsorption, corrosion inhibitor, corrosion rate, organic inhibitor, self-assembled, surface tension

INTRODUCTION

Corrosion inhibitors are frequently used as an economic and effective strategy to mitigate internal corrosion of mild steel pipelines. Consideration of internal pipeline corrosion is critically important to the oil and gas industry, be it for management of asset integrity, safety, environmental protection, or prevention of economic consequences of failure. Much research has been conducted to evaluate the corrosion mechanisms involved in so-called “sweet” systems, with aqueous CO₂,¹⁻³ more neglected was research evaluating corrosion mechanisms in the presence of organic corrosion inhibitors, although this topic has been receiving more attention in recent years.⁴⁻⁹ Organic corrosion inhibitors have a structure similar to that of surfactants, consisting of a polar/hydrophilic head group, by which they can adsorb to the steel surface, and a nonpolar/hydrophobic tail that forms a hydrophobic barrier. When a surfactant inhibitor film forms on a metal surface, this results in decreased corrosion rates.⁸⁻¹⁰ The properties of such surfactant-type inhibitor molecules, their structures, and behavior in aqueous solutions have been investigated for many years in order to understand their behavior, as well as improve their inhibition efficiency. One of the parameters related to the behavior of these inhibitors is their so-called critical micelle concentration (CMC), which is the concentration when these surfactant-type molecules begin to aggregate into structures called micelles in the bulk solution. The CMC is one of the frequently used parameters for determining the injection dosage rate of an inhibitor under

field conditions for a number of reasons as discussed below.¹¹

Micelle formation is considered as an important measurable property of surfactant corrosion inhibitors. The solubility of surfactant molecules in water at different concentrations is based on the nature of the hydrophobic part of their structure—the nonpolar tail. When the alkyl tail length is short, then discrete, unaggregated molecules dissolve in water with a small increase in free energy of solvation, as this just requires reconfiguration of water molecules around the smaller molecule rather than breaking the hydrogen bonds between water molecules.¹² As the tail length of the surfactant increases, the volume that each molecule occupies requires the breaking of the hydrogen bonds (increases in free energy) which eventually results in water molecules being repelled by the hydrophobic part of the surfactant molecules. Therefore, as the concentration of the surfactant having long tail length increases in water, with the smallest interface between water and the hydrophobic part of the molecules being thermodynamically favored, the free energy of the system increases. To reduce the free energy, two different outcomes can be expected:¹²⁻¹⁴

- The surfactant molecules will increasingly migrate to the water/air or water/oil interface⁽¹⁾ oriented with the polar head in the water and the nonpolar tail in the air or oil phase until saturation at the interface is approached.¹³⁻¹⁴
- The surfactant molecules will start aggregating in the solution once the saturation concentration is exceeded in order to minimize the interface between the nonpolar

Submitted for publication: September 2, 2020. Revised and accepted: November 21, 2020. Preprint available online: November 21, 2020, <https://doi.org/10.5006/3679>.

[‡] Corresponding author. E-mail: nm867515@ohio.edu.

^{*} Institute for Corrosion and Multiphase Technology, Department of Chemical and Biomolecular Engineering, Ohio University, Athens, Ohio 45701.

⁽¹⁾ When it comes to the boundary between water and gas phases, the words *interface* and *surface* are used interchangeably in this paper. That is: *water surface* means the same as the *water/gas interface*. Likewise, *surface tension* means the same as *water/gas interfacial tension*.

tails of the surfactant and water molecules. The surfactant molecules reorient in a way that the nonpolar tails are turned "inward" (toward each other) and the polar heads face the polar water molecules. This results in the formation of micelles as a thermodynamically favored arrangement with a smaller free energy.¹²⁻¹⁴

When it comes to corrosion, another interface is introduced into the picture, one which is key to the overall argument presented in this paper—metal surface. This results in:

- The surfactant molecules adsorbing at the metal surface with the polar/hydrophilic head group facing the metal and the nonpolar/hydrophobic tail facing the solution.

It has been argued that at or above the CMC the corroding metal surface is covered by these adsorbed molecules^{9,15} and will reach a maximum level of corrosion inhibition. Moreover, many studies claim that once the CMC has been exceeded, and the maximum decrease in corrosion rate has been achieved, the addition of more surfactant inhibitor would only result in the formation of more micelles in the bulk solution rather than having them increasingly adsorb on the metal surface.^{11,16-17} However, there is increasing evidence that the situation is not so simple. For example: an atomic force microscopy (AFM) study using a cationic surfactant, 1-dodecylpyridinium chloride, found that a carbon steel surface was entirely covered by this corrosion inhibitor at 1 CMC with the corresponding inhibition efficiency of about 70%, while at 9 CMC it reached an inhibition efficiency of about 90%.⁹ This and some other similar observations suggest that the assumed link between CMC and inhibition efficiency requires further investigation.

The easiest and most common method for determining CMC is via surface tension measurement at the water-air interface.^{15,18} The idea is that as a surfactant concentration increases in an aqueous solution, the measured interfacial tension decreases until it reaches a plateau and, at that point, the CMC is found. However, this behavior gives rise to at least two plausible hypotheses, which could explain it:

- **Hypothesis no. 1: the water/air interface saturates with the surfactant molecules when the surface tension reaches the plateau.** With increasing concentrations of surfactant molecules in a solution, the amount of surfactant molecules at the water/air interface increases until it reaches saturation and the measured surface tension approaches a plateau, while at the same time the saturation in the bulk solution has not been reached and the micelles did not form.
- **Hypothesis no. 2: the bulk solution reaches saturation with the surfactant molecules and micelles are formed.** The concentration of the surfactants in the bulk solution increases until it becomes saturated when micelles begin to form, while at the same time the saturation of the water/air interface has not been reached.

Both hypotheses are consistent with reaching a plateau in surface tension measurements at some concentration, but only if hypothesis no. 2 is true can the CMC of the surfactant be determined this way. In that case, any further addition of the surfactant beyond the CMC would result in the formation of more micelles rather than having the surfactant accumulate at the water/air interface. However, hypothesis no. 1 is a classical explanation that underpins adsorption isotherms and cannot be

rejected lightly. Therefore, an alternative, independent method to measure CMC is required, in order to distinguish which hypothesis holds true.⁽²⁾

The overall scenario behind the CMC being a critical parameter in corrosion inhibition gives rise to one more hypothesis that can be postulated:

- **Hypothesis no. 3: the maximum corrosion inhibition efficiency is achieved when the metal surface reaches a certain coverage by the inhibitor, which corresponds to the bulk CMC.** The CMC can be determined by the plateau in the surface tension measurements at the water/air interface or by an alternative technique.

In summary, these three hypotheses postulate that the behavior at one interface (corrosion at the metal surface) is related to what is occurring in the bulk (formation of micelles) by measuring what is occurring at another interface (changes in water/air interfacial tension). Whether this is true (or not) can only be determined if the surfactant inhibitor concentrations obtained at the plateau of water/air interfacial tension corresponds to the independently measured CMC in the bulk solution and also corresponds to the independently determined inhibitor concentration at which maximum corrosion inhibition efficiency is found.

Therefore, the primary objective of this research was to evaluate the validity of the surface tension measurement for determining CMC, as a means of identifying optimal corrosion inhibitor concentration. For surface tension measurement, the standard Du Noüy ring method was used; for determination of the CMC of the surfactant inhibitor molecules, amongst the 70+ techniques identified in the open literature,¹⁸ one of the most common ones—the fluorescence spectroscopy—was used. In fluorescence spectroscopy, a fluorophore is used, which can be excited to emit light more in a nonpolar environment compared to a polar environment.¹⁹⁻²⁰ The emission intensity emitted from a fluorophore molecule is related to the extent of hydrophobicity of its immediate environment. Therefore, the fluorophore molecule is almost nonfluorescent in water or other polar solvents. Below the CMC, when only discrete inhibitor molecules are present in an aqueous solution and hydrophobicity of the medium is low, fluorophore molecule fluoresces to a low extent in this polar solvent. However, when micelles form, the interior part of the micelle becomes a hydrophobic microenvironment from which the fluorophore molecule will emit light with higher intensity. Therefore, the measurement of the intensity of emitted light can be readily used to detect and quantify the formation of micelles.^{19,21} Meanwhile, the emission intensity of the fluorophore molecules is influenced by several parameters such as solvent polarity, viscosity, temperature, presence of impurities, etc.²² It should be noted that the fluorescence spectroscopy techniques provide information only about the bulk solution and do not directly relate to anything that may be happening at the metal/liquid interface. Therefore, to evaluate the adsorption of the corrosion inhibitors on the metal surface and their inhibition efficiency, electrochemical methods were used.

EXPERIMENTAL PROCEDURES

2.1 | Synthesis of the Surfactant Inhibitor Model Compounds

Benzyltrimethylalkylammonium bromide surfactant inhibitor model compounds were synthesized, with systematically increasing alkyl tail lengths, as shown Figure 1 (C# refers to

⁽²⁾ Here it is assumed that the likelihood of both hypotheses being true is low, i.e., that the water/air interface and the solution become saturated at the same concentration is highly improbable.

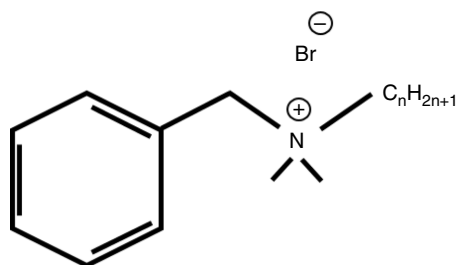


FIGURE 1. Chemical structure of the benzyltrimethylalkylammonium bromide inhibitor model compounds.

Table 1. Test Matrix for the Synthesis of the Inhibitor Model Compounds

Parameter	Value
Inhibitor model compounds	C6, C8, C10, C12, and C14
N,N-dimethylbenzylamine	0.1 mol
Alkyl bromide	0.1 mol
Acetonitrile	100 mL
Time	24 h
Reflux temperature	82°C

the number of carbon atoms in the alkyl tail of the synthesized molecules⁽³⁾. Table 1 shows the test conditions for the synthesis of the model compounds. Initially, N,N-dimethylbenzylamine was mixed with acetonitrile (solvent) in a two-necked round-bottomed flask (24/29 joints) which was then brought to reflux temperature (ca. 82°C). Next, the appropriate alkyl bromide reagent was added dropwise to the mixture using an addition funnel. The temperature of the mixture was readjusted to the reflux temperature using a heating mantle connected to a Variac[†]. The fitted condenser, with a steadily maintained flow of water therein, permitted refluxing of the mixture for 24 h to ensure completion of the amine alkylation reaction. The other details related to the syntheses are provided in Table 1. In order to remove the solvent from the final product, rotary evaporation was used while slowly increasing the temperature of the water bath to 100°C. This, along with vacuum, facilitated the complete vaporization of the solvent from the product, as well as any residual reactants. The final products were characterized using ¹H-NMR spectroscopy and melting point determination.

2.2 | Surface Tension Measurement

The surface tension experiments were performed with aqueous solutions at different concentrations of the inhibitor. A concentrated inhibitor solution was dissolved in deionized (DI) water to achieve the desired concentration and at various salinities: 0, 1 wt%, and 10 wt% NaCl concentrations. The temperature of the solutions was adjusted to 30°C using a water bath. For the surface tension measurements, the Du Noüy ring method was used, using a semiautomatic Krüss K20[†] tensiometer. The Du Noüy ring was decontaminated in between

measurements by sequentially cleaning with acetone, DI water, and a propane flame. To examine if there is any effect of the dissolved CO₂ on the CMC of the inhibitors, for one of the inhibitors (C14) the solution was sparged with CO₂ gas at 1 bar and for 1 h and surface tension was measured again. All of the measurements were repeated at least three times.

2.3 | Fluorescence Spectroscopy Measurement

Nile Red was used as the fluorescence probe in this testing because of its reported accuracy for detecting micelles of the quaternary ammonium bromide molecules used as corrosion inhibitors in the current work.²¹ The fluorescence spectroscopy measurements were performed at the same conditions as were used for the surface tension measurements and repeated at least twice to confirm the accuracy of the results using a Fluorolog 3-FLC 21[†] spectrofluorometer, manufactured by Horiba Instruments (Edison, NJ). Nile red was purchased from Molecular Probes⁽⁴⁾ or Acros Organics⁽⁵⁾. Dimethyl sulfoxide (DMSO) from Fisher Scientific⁽⁶⁾ was used as a nonpolar solvent for Nile Red powder. Initially, the Nile Red was dissolved and stirred in DMSO in the ratio of 1 mg/mL in order to be able to add it to water.

2.4 | Corrosion Rate Measurement

Linear polarization resistance (LPR) corrosion rate measurements were performed for each inhibitor at different concentrations (Table 2) to find the concentration corresponding to the maximum efficiencies of the inhibitors. The inhibitor concentration at which the maximum decrease in corrosion rate was achieved is defined here as the metal surface saturation concentration, which is described in more detail elsewhere.^{5,23} A 2 L glass cell filled with 1 wt% NaCl and at 30±0.5°C was sparged with 1 bar CO₂ for 2 h to remove dissolved oxygen. The pH of the solution was adjusted to 4.00±0.01 using a deoxygenated dilute NaOH solution. The working electrode was an API 5L X65 rotating cylinder electrode (RCE) with a rotating speed of 1,000 rpm. The steel surface of the specimen was polished with sandpaper up to 600 grit, cleaned with isopropanol in an ultrasonic bath, and dried with a nitrogen gas stream. A saturated Ag/AgCl electrode and platinum covered titanium mesh were used as reference and counter electrodes, respectively. Measurements were performed by scanning from -5 mV_{OCF} to +5 mV_{OCF} and the corrosion rate was obtained from the measured polarization resistance using a B value of 26 mV/decade.

RESULTS AND DISCUSSION

3.1 | Analysis of the Synthesized Inhibitor Model Compounds

Quaternary ammonium bromide inhibitor model compounds were synthesized. C6, like C4, had a crystalline solid

Table 2. Types and Concentration (ppm by Mass) of Quaternary Ammonium Bromide Model Inhibitors Used

Compounds	Concentration (ppm mg/L)
C4	10, 50, 100, 150, 200, 250, and 300
C8	10, 50, 100, 150, 200, and 250
C12	10, 50, 100, 150, and 200
C14	5, 10, 25, 50, and 100
C16	5, 10, 25, and 50

⁽³⁾ Synthesis of C4 and C16 used in this work were conducted previously by Juan Dominguez Olivo as part of a different study.⁵

[†] Trade name.

⁽⁴⁾ Molecular Probes, Inc.

⁽⁵⁾ www.acros.com.

⁽⁶⁾ www.fishersci.com.

Table 3. Melting Point of the Synthesized Inhibitor Model Compounds

Compound	Melting Point Range (°C)
C4	148–50.5
C6	120.0–121.9
C14	63.7–67.0
C16	73.3–80

structure, while C8, C10, and C12 were ionic liquids. However, C14, like C16, existed as a waxy solid.^{5,24} ¹H-NMR spectral analysis of the products indicated that the synthesized components were free of the reactants and the solvent. Moreover, it confirmed that the model compounds have the correct structure and are of high purity (+99.5%) as shown elsewhere.^{5,24} The range of the melting points for the crystallin model compounds (C4 and C6) and waxy solids model compounds (C14 and C16) are shown in Table 3.

3.2 | Surface Tension Measurements

The first step was to establish if the surface tension measurements were affected by the nature of the dissolved gas, so the effect of the dissolved CO₂ on the CMC of C14 was examined. The surface tension was measured at progressively higher inhibitor concentrations until an inflection in the curve of surface tension vs. inhibitor concentration was observed. As shown in Figure 2, the saturation values for both solutions were approximately the same, which indicated that the presence of CO₂ did not affect the accumulation of the inhibitor molecules at the water/gas interface and all subsequent measurements were done in air, which was much less cumbersome. These measurements were repeated twice with good accuracy, as shown in Figure 2. In the text below, the inhibitor concentration at which the inflection point in the curve of surface tension vs. inhibitor concentration is observed will be called the water/air interfacial saturation concentration (W-AISC).

Surface tension measurements of the inhibitor model compounds with different alkyl tail lengths are shown in Figures 3, 4, and 5 for solutions with 0, 1 wt%, and 10 wt% NaCl

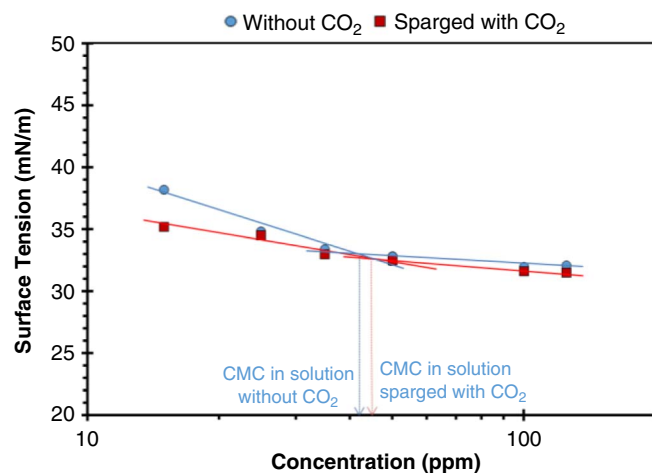


FIGURE 2. Water/gas interfacial saturation concentration for the C14 corrosion inhibitor in 1 wt% NaCl solution with and without dissolved CO₂ gas and at 30°C. Error bars obtained from duplicate measurements are smaller than the data markers.

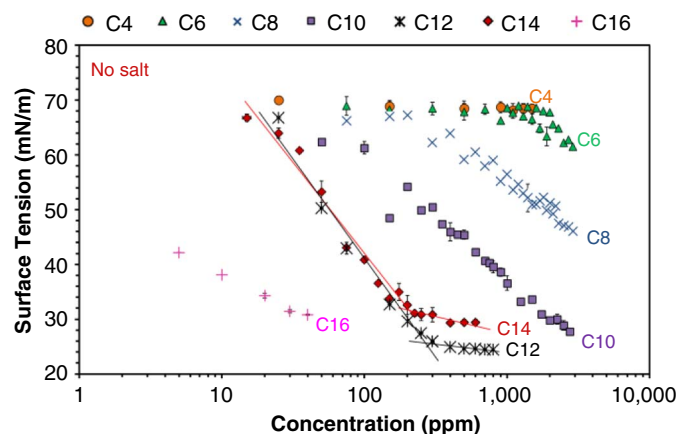


FIGURE 3. Surface tension vs. concentration curves used for determination of the water/air interfacial saturation concentration (W-AISC) in solutions without NaCl and at 30°C. Error bars show the minimum and maximum values obtained from multiple measurements.

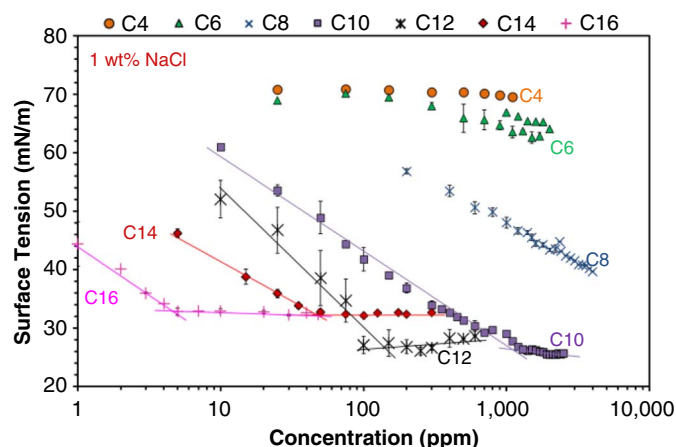


FIGURE 4. Surface tension vs. concentration curves used for determination of the water/air interfacial saturation concentration (W-AISC) in 1 wt% NaCl aqueous solution and at 30°C. Error bars show the minimum and maximum values obtained from multiple measurements.

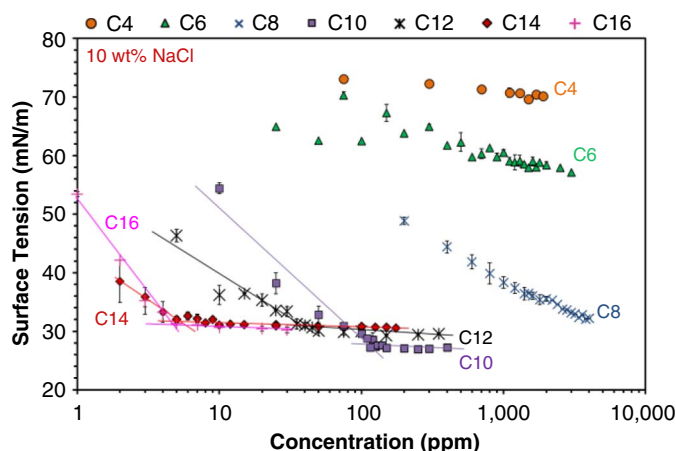


FIGURE 5. Surface tension vs. concentration curves used for determination of the water/air interfacial saturation concentration (W-AISC) in 10 wt% NaCl aqueous solution and at 30°C. Error bars show the minimum and maximum values obtained from multiple measurements.

concentrations, respectively. In a solution without any salt, the presence of C4 and C6 inhibitors in concentrations up to 3,000 ppm did not significantly change the surface tension of water. This can be explained by the short tail length of these molecules which did not influence the free energy of the system sufficiently to force them to accumulate at the water/air interface in measurable quantities. For larger inhibitor molecules, C8 and C10, the surface tension of DI water decreased with the increase in inhibitor concentration up to 3,000 ppm, but it did not reach a plateau, required to determine the W-AISC. Larger inhibitor molecules, C12 and C14, decreased the surface tension until a plateau in surface tension was seen and an inflection point could be identified. The largest inhibitor molecule (C16) has a very low solubility in water, which limited the measurements to concentrations below 50 ppm. In this range, the most dramatic decrease in surface tension was observed at low concentrations, but no clear inflection point in the surface tension curve could be identified.

In addition, the effect of salt concentration on this behavior was investigated. The C4, C6, and C8 inhibitors did not exhibit a plateau at any salt concentration tested here and an

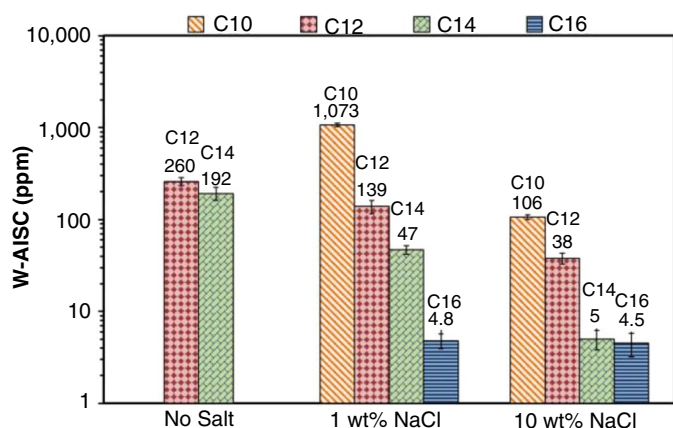


FIGURE 6. Comparison of water/air interfacial saturation concentration (W-AISC) obtained at different tail lengths of the inhibitor model compounds in solutions with different salinity and at 30°C. Error bars show the variability obtained from multiple experiments.

inflection point could not be identified. However, the C10 inhibitor compound which did not show a plateau in a solution without any salt exhibited it at salt concentrations of 1 wt% and 10 wt%. Moreover, the increase in salt concentration decreased the W-AISC for C10, C12, C14, and C16 determined by the shift in the position of the inflection point. Figure 6 and Table 4 show the summary of the obtained W-AISC values for different salt concentrations and tail lengths of the inhibitor model compounds. As is clearly seen in Figure 6, by increasing the tail length of the inhibitor compounds from C4 to C16, the W-AISC decreased. The same is true when it comes to increased salt concentrations which decreased the measured W-AISC.

While the measurements presented above seem to generally fit with the understanding that surface tension should decrease with an addition of a surfactant until a plateau is reached, they do not enable distinguishing between the two possible explanations and therefore neither hypothesis no. 2 nor hypothesis no. 1 could be confirmed/rejected. However, one additional observation needs to be emphasized. Irrespective of the chain length, the plateau in the surface tension measurements was always reached at a similar magnitude, somewhere around 30 mN/m. This was true in all inhibitor solutions where the plateau was detected, with or without salt, and indicates a similar state of the water/air interface when it comes to the accumulation of the inhibitor. One can deduce that the most likely explanation for this would be that in all cases the surface became saturated with the inhibitor in more or less the same way, albeit at progressively lower bulk concentrations for larger molecules, which seems to be favoring hypothesis no. 1. However, the validity of hypothesis no. 2 and the feasibility of surface tension measurement as an indirect method for the detection of CMC was further tested by comparing the W-AISC with the CMCs obtained by the alternative method, fluorescence spectroscopy.

3.3 | Fluorescence Spectroscopy Measurements

An example of the raw fluorescence spectroscopy data for C16 in 1 wt% NaCl solution is shown in Figure 7 on the left. Until 15 ppm of inhibitor was added, no peak in emission intensity could be observed. At 15 ppm and higher concentrations, a peak is observed at an emission wavelength of approximately 640 ± 1 nm. This is clearly indicated in the related

Table 4. Measurement of the Critical Micelle Concentration (CMC) by Fluorescence Spectroscopy and Water/Air Interfacial Saturation Concentration (W-AISC) by Surface Tension Measurements, for Inhibitor Model Compounds with Different Tail Lengths Dissolved in Aqueous Solutions with Different Salinity and at 30°C^(A)

Inhibitor Model Compound	Salt Content					
	No Salt		1 wt% NaCl		10 wt% NaCl	
	W-AISC	CMC	W-AISC	CMC	W-AISC	CMC
C4	>1,500	Not measured	>1,000	>5,000	>2,000	Not measured
C6	>3,000	Not measured	>2,000	>4,000	>3,000	Not measured
C8	>3,000	Not measured	>4,000	>4,000	>4,000	Not measured
C10	>3,000	>3,000	1,073 ± 50	1,431 ± 142	106 ± 6	162 ± 24
C12	260 ± 25	504 ± 25	139 ± 23	345 ± 19	38 ± 5	81 ± 18
C14	192 ± 31	15,919	47 ± 5	52 ± 5	5 ± 1.2	55 ± 5
C16	>50	>50	4.8 ± 0.9	14.3 ± 0.9	4.5 ± 1.3	8.1 ± 0.3

^(A) The reported numbers are averages and the scatter (indicating maximum and minimum values).

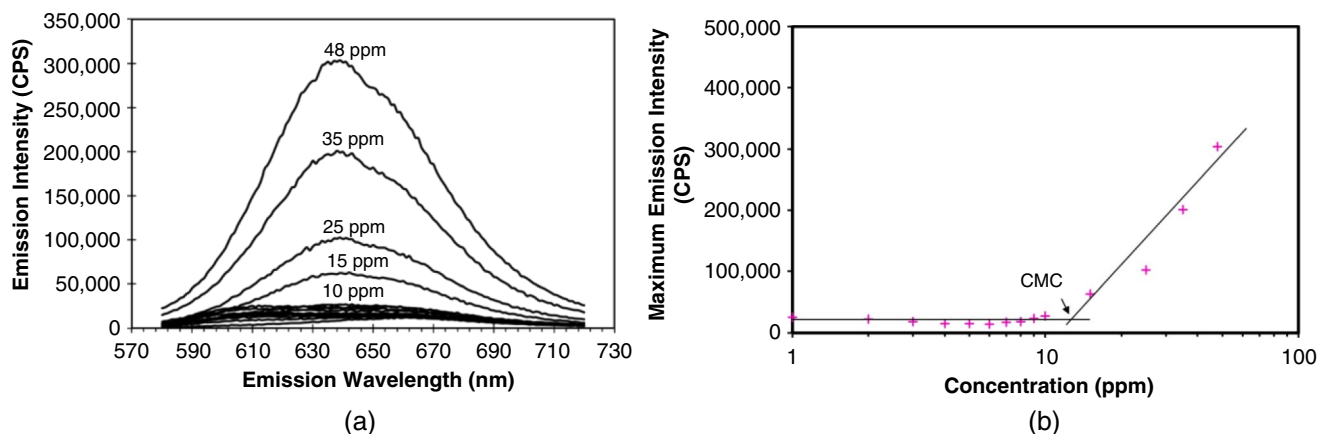


FIGURE 7. Example of fluorescence spectroscopy results for C16 inhibitor in a 1 wt% NaCl aqueous solution and at 30°C: (a) raw emission intensity data and (b) peak emission intensity as a function of inhibitor concentration.

graph showing the maximum emission intensity vs. concentration in Figure 7. Therefore, it can be concluded that somewhere between 10 ppm and 15 ppm of the C16 inhibitor concentration in solution micelles started to form and this could be taken as the CMC.

Figure 8 shows the fluorescence spectroscopy results for C4, C6, and C8 in a 1 wt% NaCl solution. These results show that micelles did not form in these solutions, as no clear increase in peak emission intensity can be observed for any of these inhibitors. There is some increase in peak intensity at around 3,000 ppm for C6 and around 800 ppm for C8, but this is not conclusive. Overall, these results are in broad agreement with the results of the surface tension measurement technique. Figure 9 shows the fluorescence spectroscopy results for C10, C12, C14, and C16 in 1 wt% NaCl, where the CMC value could be found and is reported when the first significant change in emission intensity is measured. The same measurements were performed for solutions having no salt and 10 wt% NaCl and are shown in Table 4.

3.4 | Comparison of the Water/Air Interfacial Saturation Concentration and Critical Micelle Concentration

The above data provided the means to determine whether hypothesis no. 1 or hypothesis no. 2 are true, i.e., whether CMC can be properly determined by using surface tension measurements. Figure 10 shows the comparisons between W-AISC obtained by surface tension measurements and CMC obtained by fluorescence spectroscopy with respect to the salt concentration and alkyl tail length. It is clear that the concentration values obtained by the two techniques are of the same order of magnitude. Furthermore, both techniques show a decrease in the measured concentration with increased inhibitor tail length, as would be expected. In two of ten cases, the measured W-AISC and CMC are the same, i.e., the observed differences are within the range of measurement errors (C14 in pure water and 1 wt% NaCl solution). However, for the other eight cases, the CMC measured by fluorescence spectroscopy is higher than the W-AISC determined by surface tension measurements by a large margin—a factor of two or even three. While these observations are not entirely conclusive, they lend more support to hypothesis no. 1, rather than hypothesis no. 2. That is, the quaternary ammonium model compounds used in this study first saturate the water/air surface before they saturate the bulk solution leading to micelle formation.

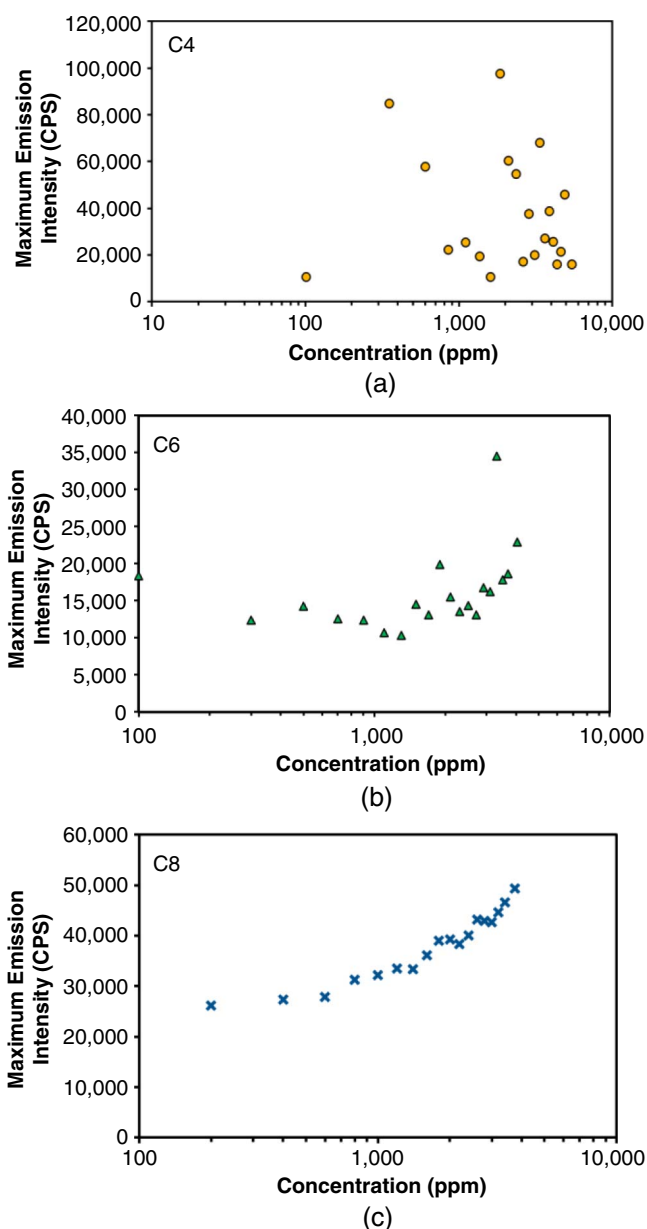


FIGURE 8. Fluorescence spectroscopy results for C4, C6, and C8 in 1 wt% NaCl solution and at 30°C.

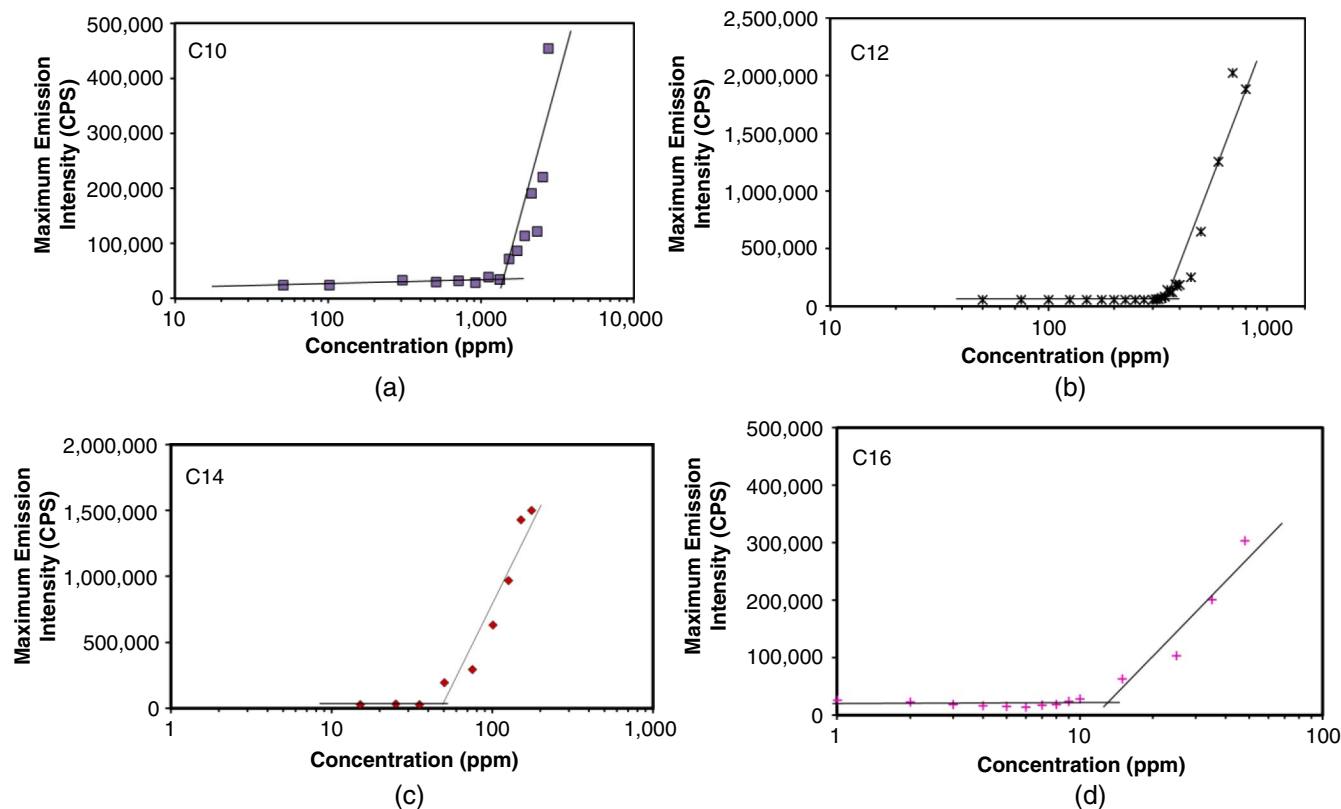


FIGURE 9. CMC of C10, C12, C14, and C16 inhibitor aqueous solutions with 1 wt% NaCl and at 30°C based on fluorescence spectroscopy measurements.

The effect of salt also provides support for hypothesis no. 1, and here is the reasoning behind it. It was already established that the addition of a surfactant inhibitor normally results in the accumulation of the inhibitor molecules on the water/air interface because of the nonpolar tails of inhibitor molecules being repelled by the polar aqueous environment; adding salt to the solution does not change this situation much, the inhibitor molecules are still repelled from the bulk water toward the water/air interface more or less in the same way. However, at the water/air interface the positive head groups of the inhibitor molecules repel each other, which limits the number of inhibitor molecules that can fit there. Adding NaCl leads to an interaction between the positive head group of the inhibitor and the negative chloride ions what decreases the repulsion forces between the charged inhibitor molecule head groups accumulated at the water/air interface. In other words, in the presence of salt, the inhibitor molecules become more stable near each other at the water/air interface, allowing more of them to be packed there for the same bulk inhibitor concentration. This can be seen by comparing the surface tension of water at a constant bulk concentration of inhibitor and in different salt solutions, as shown by the example of C12 in Figure 11. There, it can be seen that at the same inhibitor concentration, the surface tension is lowered in the presence of salt because more inhibitor molecules are able to accumulate at the water/air interface. For the same reason, the water/air interface saturation occurs at lower bulk inhibitor concentrations²⁵⁻²⁷ in the presence of salt and the W-AISC decreases, as shown for the example of C12 in Figure 12. This ability of salt to decrease the repulsion forces between the positive head group of inhibitors when in close proximity also helps with formation of micelles, also shown in Figure 12.²⁶⁻²⁷

3.5 | Corrosion Rate Measurements

In addition to the CMC related to bulk saturation, and W-AISC related to water/air surface saturation, a comparison is now introduced to a related measure of inhibitor concentration related to corrosion—the so-called metal surface saturation concentration (MSSC). It is defined as the corrosion inhibitor concentration at which any further addition of inhibitor to the solution does not decrease the corrosion rate or, in other words, a bulk inhibitor concentration when a maximum coverage by the corrosion inhibitor on the corroding surface is reached.^{5,23} It is important to mention that this concentration may or may not correspond to full coverage of the metal surface.

The relationship between the micelle formation in the bulk (at CMC), adsorption of the inhibitors at the water/air interface (W-AISC), and the formation of inhibitor films at the metal surface (at MSSC) is still not understood. Therefore, the MSSC was determined independently and compared with CMC and W-AISC. To obtain the MSSC, electrochemical corrosion rate measurements were performed at different concentrations of the inhibitor model compounds. The concentration beyond which a further decrease in corrosion rate did not occur was considered to be a measure of MSSC, i.e., the concentration at which maximum coverage by the corrosion inhibitor occurred.⁵ All of the measurements with the above-mentioned inhibitor model compounds were performed in a CO₂ saturated, 1 wt% NaCl solution at pH 4.0 and temperature of 30°C.

An example of the experimental results and analysis for C14 is shown in Figure 13 where it is shown that with an increase in corrosion inhibitor concentration up to 50 ppm the stable corrosion rate is progressively smaller. However, above 50 ppm

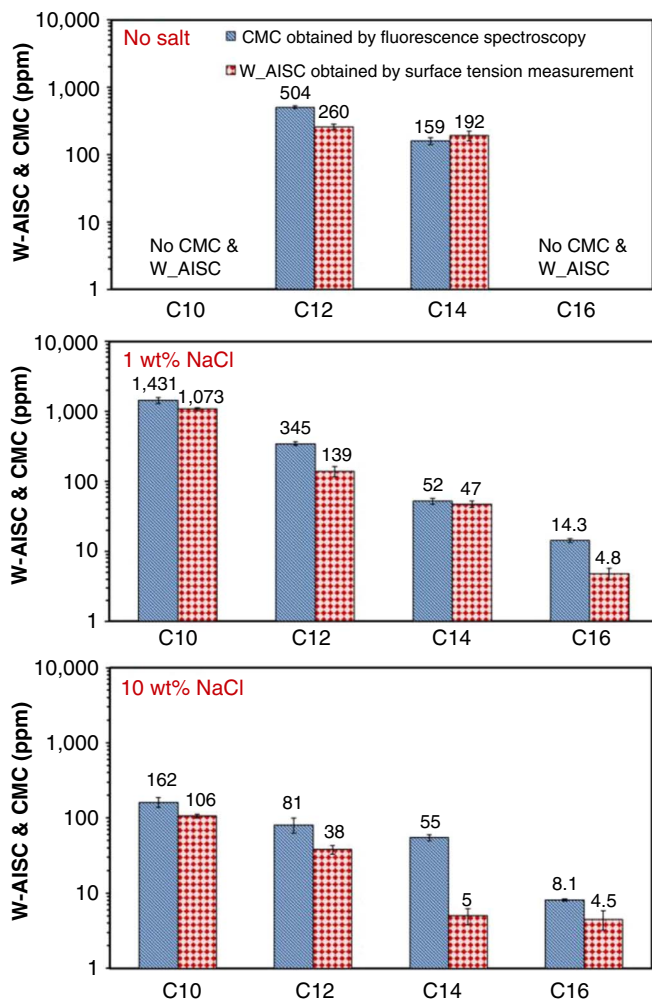


FIGURE 10. Comparison of CMCs obtained by fluorescence spectroscopy and surface tension measurements in aqueous solutions having no salt, 1 wt% NaCl, and 10 wt% NaCl and at 30°C. The reported numbers are average values and the error bars show the minimum and maximum values obtained.

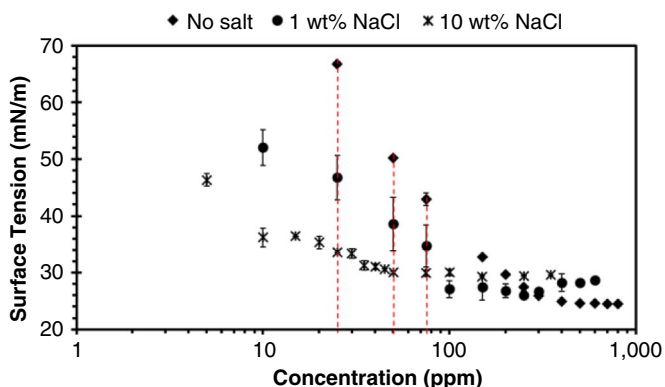


FIGURE 11. Surface tension measurements of C12 in aqueous solutions having no salt, 1 wt% NaCl, and 10 wt% NaCl, and at 30°C. Red dotted lines represent locations where surface tensions were measured at the same inhibitor concentration. Error bars show the minimum and maximum values obtained.

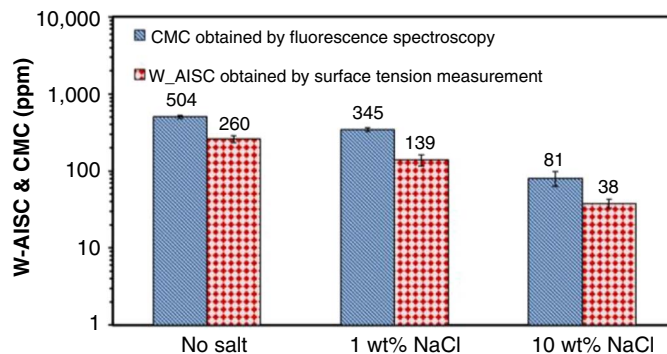


FIGURE 12. Effect of salt concentration on the CMC and W-AISC of C12 obtained by the two independent techniques. The reported numbers are average values and the error bars show the minimum and maximum values obtained.

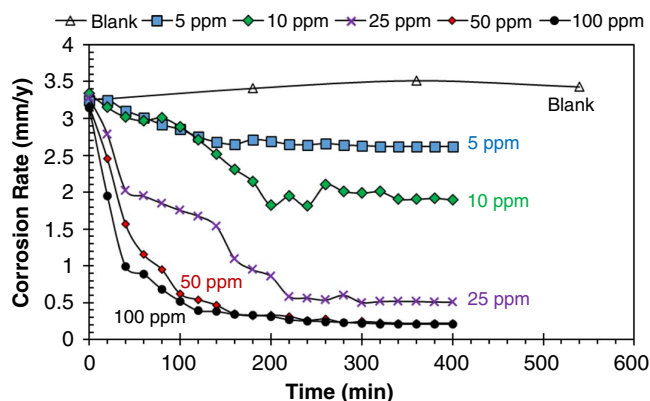


FIGURE 13. Determining the metal surface saturation by electrochemical corrosion rate measurements with different concentrations of C14 inhibitor, in a 1 wt% NaCl aqueous solution, 1 bar CO₂, pH 4, and at 30°C.

the stable corrosion rate does not change with concentration anymore, which suggests that the adsorbed inhibitor molecules are providing the maximum coverage of the metal surface at bulk concentrations somewhere between 25 ppm and 50 ppm.

The W-AISC obtained by surface tension measurements, the CMC obtained by fluorescence spectroscopy and the MSSC obtained by electrochemical corrosion measurements are compared in Figure 14 and summarized in Table 5. The following observations can be made:

- For the C4 and C8 inhibitors, there was no measurable W-AISC by surface tension measurements and no measurable CMC by fluorescence spectroscopy, i.e., they did not reach saturation either at the metal surface or the bulk solution, yet it was possible to determine their MSSC by electrochemical corrosion rate measurements, somewhere in the range 100 ppm to 200 ppm.
- For C12 inhibitor, the CMC was by far the highest (345 ± 19 ppm), the W-AISC was much lower (139 ± 23 ppm), and the MSSC was in the range of 50 ppm to 100 ppm. This suggests that as the concentration of the C12 inhibitor increases in the bulk solution, the metal surface saturates first, followed by the water/air interface and finally the micelles form in the bulk solution.
- For C14, the three values are much closer. Again, the metal surface saturates first, somewhere in the range of

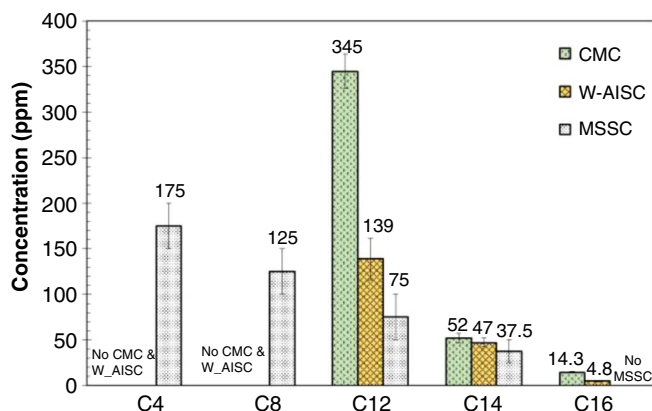


FIGURE 14. Comparison of the water/air interfacial saturation concentration (W-AISC) obtained by surface tension measurements, the critical micelle concentration (CMC) obtained by fluorescence spectroscopy, and the metal surface saturation concentration (MSSC) obtained by electrochemical corrosion measurements for model inhibitor compounds in an aqueous solution with 1 wt% NaCl, 1 bar CO₂, pH 4, and 30°C. The reported numbers are average values and the error bars show the minimum and maximum values obtained.

25 ppm to 50 ppm, while the water/interface and the bulk solution reach saturation somewhere around 47 ppm and 52 ppm, respectively, so all three values are quite similar.

- For C16, the MSSC could not be found within the range of solubility for this inhibitor (0 to 50 ppm) and it was concluded that the metal surface possibly reaches saturation at concentrations higher than 50 ppm. Meanwhile, the saturation of the water/air surface happened in the concentration range 4.8±0.9 ppm while the micelles formed for concentrations more than twice as high, i.e., CMC was in the range 14.3±0.9 ppm. This suggests that the large inhibitor molecule C16 has a relatively poor affinity for adsorption onto the metal surface when compared to the propensity to accumulate at the water/air interface and the tendency to form micelles in the bulk solution.

From this, it can be concluded that there is no universal relationship between the A-WISC, CMC, and MSSC, and that one of those cannot be measured and assumed to be equal to the others. The relationship between the three measure values

depends on the inhibitor molecule. The smaller inhibitor molecules (C4, C8, and C12) have shown a stronger tendency to adsorb at the metal surface than to accumulate at the water/air interface or form micelles in the bulk solution. For C14, this tendency is approximately the same while the large C16 molecule has shown that it will rather migrate to the water/air interface or form micelles than adsorb onto the metal surface.

Returning to the original hypotheses, the following can be stated:

- Hypothesis no. 1 is true.** When the measured surface tension reaches the plateau, this means that the water/air interface is saturated by the surfactant molecules.
- Hypothesis no. 2 is false.** When the measured surface tension reaches the plateau, this does not necessarily mean that the bulk solution reached saturation with the surfactant molecules and that micelles formed.
- Hypothesis no. 3 is also false.** There is no universal relationship between the CMC (the saturation of the bulk solution with the inhibitor) and the maximum corrosion inhibition efficiency achieved at a certain coverage by the adsorbed inhibitor.

The practical implication of this research is the realization that CMC cannot be reliably determined by the surface tension measurements at the water/air interface. Furthermore, when determined by a more suitable alternative technique such as fluorescence spectroscopy, the CMC cannot be used to find the optimal corrosion inhibitor concentration that will result in maximum protection.

CONCLUSIONS

- Analyses revealed that for the synthesized inhibitor compounds, first, the water/air interface became saturated and then, at higher concentration, micelles started to form in the bulk. Consequently, using surface tension measurement gave information about the concentration at which the water surface became saturated instead of data that could be used for determination of CMC. This means that the surface tension measurement normally used for determining CMC is not an adequate technique. This technique measures the water surface tension which may or may not have a relationship to the formation of micelles in the bulk solution.
- Using fluorescence spectroscopy, for the inhibitors model compounds which form micelles in the tested aqueous solution, it

Table 5. Measured Values of the Water/Air Interfacial Saturation Concentration (W-AISC) Obtained by Surface Tension Measurements, the Critical Micelle Concentration (CMC) Obtained by Fluorescence Spectroscopy, and the Metal Surface Saturation Concentration (MSSC) Obtained by Electrochemical Corrosion Measurements for Model Inhibitor Compounds in an Aqueous Solution Having 1 wt% NaCl, 1 bar CO₂, pH4, and at 30°C^(A)

Inhibitor Model Compound	W-AISC (ppm)	CMC (ppm)	MSSC (ppm)	Stable Corrosion Rate (mm/y)	Inhibition Efficiency
Blank	–	–	–	3.14	–
C4	>1,000	>5,000	150–200	1.15	63%
C8	>4,000	>4,000	100–150	0.69	78%
C12	139±23	345±19	50–100	0.38	88%
C14	47±5	52±5	25–50	0.22	93%
C16	4.8±0.9	14.3±0.9	>50	0.15	95%

^(A) The reported numbers are averages and the scatter (indicating maximum and minimum values).

was shown that by increasing the alkyl tail length of the inhibitor or the salt concentration of the bulk solution CMC decreased. Some of the inhibitors with short tail length did not form micelles even in the highly concentrated NaCl aqueous electrolytes.

➤ Maximum inhibition efficiency determined by individual electrochemical corrosion rate experiments at increasing inhibitor concentrations (defined as the metal surface saturation concentration) did not show any specific relationship to the CMC.

➤ It was shown for the synthesized inhibitor compounds C4 and C8, that even if these corrosion inhibitors did not have a measurable CMC value, they provided corrosion mitigation and had a measurable metal surface saturation concentration.

ACKNOWLEDGMENTS

The authors would like to acknowledge the financial support from the following companies: Anadarko, Baker Hughes, BP, Chevron, CNOOC, ConocoPhillips, DNV GL, ExxonMobil, M-I SWACO (Schlumberger), Multi-Chem (Halliburton), Occidental Oil Company, PTT, Saudi Aramco, SINOPEC (China Petroleum), and Total.

References

1. A. Kahyarian, M. Singer, S. Nešić, *J. Nat. Gas Sci. Eng.* 29 (2016): p. 530-549.
2. A. Kahyarian, B. Brown, S. Nešić, "Fundamental Mechanisms of Mild Steel Corrosion in H₂S Containing Environments," CORROSION 2019, paper no. 12875 (Houston, TX: NACE International, 2019).
3. A. Kahyarian, S. Nešić, *J. Electrochem. Soc.* 166 (2019): p. C3048-C3063.
4. J.M. Domínguez Olivo, B. Brown, S. Nešić, "Modeling of Corrosion Mechanisms in the Presence of Quaternary Ammonium Chloride and Imidazoline Corrosion Inhibitors," CORROSION 2016, paper no. 7406 (Houston, TX: NACE, 2016).
5. J.M. Domínguez Olivo, D. Young, B. Brown, S. Nešić, "Effect of Corrosion Inhibitor Alkyl Tail Length on the Electrochemical Process Underlying CO₂ Corrosion of Mild Steel," CORROSION 2018, paper no. 11537 (Houston, TX: NACE, 2018).
6. J.M. Domínguez Olivo, B. Brown, D. Young, S. Nešić, "Electrochemical Model of CO₂ Corrosion in the Presence of Quaternary Ammonium Corrosion Inhibitor Model Compounds," CORROSION 2019, paper no. 13392 (Houston, TX: NACE, 2019).
7. Z. Belarbi, J. Dominguez Olivo, F. Farelas, M. Singer, D. Young, S. Nešić, *Corrosion* 75 (2019): p. 1246-1254.
8. Z. Belarbi, F. Farelas, M. Singer, S. Nešić, *Corrosion* 72 (2016): p. 1300-1310.
9. V. Pandarinathan, K. Lepková, S.I. Bailey, T. Becker, R. Gubner, *Ind. Eng. Chem. Res.* 53 (2014): p. 5858-5865.
10. Y. Zhu, M.L. Free, R. Woollam, W. Durnie, *Prog. Mater. Sci.* 90 (2017): p. 159-223.
11. M. Achour, J. Kolts, "Corrosion Control by Inhibition Part I: Corrosion Control by Film Forming Inhibitors," CORROSION 2015, paper no. 5475 (Houston, TX: NACE, 2015).
12. D. Chandler, *Nature* 437 (2005): p. 640-647.
13. M.J. Rosen, J.T. Kunjappu, *Surfactants and Interfacial Phenomena*, 4th ed. (Hoboken, NJ: John Wiley & Sons, Inc., 2012).
14. D. Myers, *Surfactant Science and Technology*, 3rd ed. (Hoboken, NJ: John Wiley & Sons, Inc., 2006).
15. Y. Xiong, B. Brown, B. Kinsella, S. Nešić, "AFM Studies of the Adhesion Properties of Surfactant Corrosion Inhibitor Films," CORROSION 2013, paper no. 2521 (Houston, TX: NACE, 2013).
16. M.A. Malik, M.A. Hashim, F. Nabi, S.A. AL-Thabaiti, *Int. J. Electrochem. Sci.* 6 (2011): p. 1927-1948.
17. T. Zhao, G. Mu, *Corros. Sci.* 41 (1999): p. 1937-1944.
18. P. Mukerjee, K.J. Mysels, *Critical Micelle Concentrations of Aqueous Surfactant Systems* (Washington, D.C.: National Standard Reference Data System, 1971).
19. M.C.A. Stuart, J.C. van de Pas, J.B.F.N. Engberts, *J. Phys. Org. Chem.* 18 (2005): p. 929-934.
20. I.N. Kurniasih, H. Liang, P.C. Mohr, G. Khot, J.P. Rabe, A. Mohr, *Langmuir* 31 (2015): p. 2639-2648.
21. A. Chandra, J. Vera, W. Durnie, R. Woollam, "Understanding the Relationship Between Corrosion Inhibitor Adsorption and Surfactant Properties and Micellization: Methodology," CORROSION 2018, paper no. 11467 (Houston, TX: NACE, 2018).
22. J.R. Lakowicz, *Principles of Fluorescence Spectroscopy*, 3rd ed. (New York, NY: Springer Science & Business Media, 2006).
23. T. Murakawa, S. Nagaura, N. Hackerman, *Corros. Sci.* 7 (1967): p. 79-89.
24. N. Moradighadi, S. Lewis, J.M. Domínguez Olivo, D. Young, B. Brown, S. Nešić, "Effect of Alkyl Tail Length on CMC and Mitigation Efficiency Using Model Quaternary Ammonium Corrosion Inhibitors," CORROSION 2019, paper no. 13004 (Houston, TX: NACE, 2019).
25. L.S.C. Wan, P.K.C. Poon, *J. Pharm. Sci.* 58 (1969): p. 1562-1567.
26. H. Zhou, Y. Liang, P. Huang, T. Liang, H. Wu, P. Lian, X. Leng, C. Jia, Y. Zhu, H. Jia, *J. Mol. Liquids* 249 (2018): p. 33-39.
27. D. Yu, X. Huang, M. Deng, Y. Lin, L. Jiang, J. Huang, Y. Wang, *J. Phys. Chem. B* 114 (2010): p. 14955-14964.